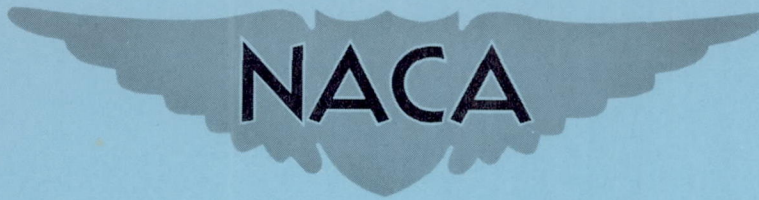


FILE COPY  
NO. 2



RM A9L29

NACA RM A9L29



# RESEARCH MEMORANDUM

TESTS OF A SMALL-SCALE NACA SUBMERGED INLET  
AT TRANSONIC MACH NUMBERS

By L. Stewart Rolls and George A. Rathert, Jr.

Ames Aeronautical Laboratory  
Moffett Field, Calif.

THIS DOCUMENT ON LOAN FROM THE FILES OF

NATIONAL ADVISORY COMMITTEE FOR AERONAUTICS  
LANGLEY AERONAUTICAL LABORATORY  
LANGLEY FIELD, HAMPTON, VIRGINIA

RETURN TO THE ABOVE ADDRESS

REQUESTS FOR PUBLICATIONS SHOULD BE ADDRESSED  
AS FOLLOWS:

NATIONAL ADVISORY COMMITTEE FOR AERONAUTICS  
1512 H STREET, N. W.  
WASHINGTON 25, D. C.

**NATIONAL ADVISORY COMMITTEE  
FOR AERONAUTICS**

WASHINGTON

February 23, 1950

NATIONAL ADVISORY COMMITTEE FOR AERONAUTICS

RESEARCH MEMORANDUM

TESTS OF A SMALL-SCALE NACA SUBMERGED INLET  
AT TRANSONIC MACH NUMBERS

By L. Stewart Rolls and George A. Rathert, Jr.

SUMMARY

The pressure-recovery characteristics at the vertical center line of an NACA submerged inlet of aspect ratio 5 have been measured in the Mach number range 0.60 to 1.08 by the wing-flow method. The variation of ram-recovery ratio determined from measurements at the center line of the inlet with test station Mach number is presented for mass-flow ratios of 0.30 to 0.60.

High ram recovery was maintained up to test-station Mach numbers of 1.03 to 1.08, where, for mass-flow ratios below 0.5, an abrupt loss in pressure recovery was associated with formation of a shock wave on the inlet ramp and subsequent interaction with ramp boundary layer.

INTRODUCTION

The favorable pressure-recovery characteristics of NACA submerged inlets have been demonstrated at low speeds (references 1 and 2) and at high subsonic speeds (reference 3). The need for data at transonic speeds on this type of inlet has become urgent due to their contemplated use on airplanes capable of flight in this range. Qualitative data at low transonic speeds have been obtained on a submerged inlet of aspect ratio 4 in a small high-speed wind tunnel (reference 4).

To provide data on a submerged inlet in the transonic range, tests were made on an aspect ratio 5 inlet using the NACA wing-flow method. This report presents the characteristics of the submerged inlet in the Mach number range of 0.60 to 1.08. The inlet characteristics are discussed solely in terms of pressure-recovery performance.

NOTATION

A duct entrance area, square feet

H	total pressure, pounds per square foot
M	Mach number
p	static pressure, pounds per square foot
V	velocity, feet per second
u	local velocity, feet per second
z	distance above test-station surface, inches
$\rho$	air density, slugs per cubic foot
$\delta$	boundary-layer thickness, inches
$\delta^*$	displacement thickness $\left[ \int_0^{\delta} \left( 1 - \frac{\rho u}{\rho_{\delta} u_{\delta}} \right) dz \right]$
$\frac{H_1 - p_0}{H_0 - p_0}$	ram-recovery ratio
$\frac{m_1}{m_0}$	mass-flow ratio $\left( \frac{\rho_1 AV_1}{\rho_0 AV_0} \right)$

#### Subscripts

o	test station (approximately 3 in. aft of 40-percent wing-chord station)
1	rake location
l	local
$\delta$	outer edge of boundary layer

#### TEST EQUIPMENT

The investigation was conducted by placing the model inlet in a region of accelerated air flow over a special built-up test station on an airplane wing. A photograph of the inlet installed on the test station is shown in figure 1. The pertinent inlet dimensions are presented in figure 2 and provide the standard divergent wall as described in reference 1. The standard type lip for this type inlet was not used on this model.

## Flow Field

Measured characteristics of the flow field include the horizontal Mach number distribution and the variation of total head through the test-station boundary layer. The measurements were made without the model installed but under conditions of constant airplane Mach number, normal acceleration, and average pressure altitude otherwise identical with the test runs. Figure 3 presents the distribution of local Mach number along the test station. The 40-percent wing chord shown on this figure locates the test station on the airplane wing. Figure 4 shows the variation at maximum airplane Mach number of total pressure through the boundary layer measured by a rake of total pressure tubes located 3 inches aft of the 40-percent wing-chord station.

## Ducting System

In producing a pressure differential across the inlet, to enable air flow through it, a ducting system was constructed whereby the discharge could be made at a region of low static pressure. The inlet exhausted into a plenum chamber which discharged through a circular duct to the upper surface of the wing at a station 33 inches inboard of the inlet. A schematic drawing of this ducting system is shown in figure 5. The amount of air flowing through the system and consequently the mass-flow ratio was varied by using several different diameter constrictions at the flow outlet.

## INSTRUMENTATION

The pressure recovery was measured by a rake of nine total pressure tubes mounted on the duct center line just inside the lip (fig. 2). The ratio of area at the measuring station to inlet area was 1.13, thus some diffusion losses were included in the measurements. The complete inlet area could not be surveyed without unduly lowering the mass-flow ratio; however, the center line measurements are considered to be a qualitative indication of the transonic characteristics of the inlet.

The mass-flow ratio was determined from a calibration of the pressure drop at the junction of the plenum chamber and the exit duct. This effective Venturi was calibrated by a series of ground tests using a compressor and a standard ASME flowmeter orifice. The location of the measuring tubes are shown in figure 5.

The static pressure distribution was measured over the forward portion of the ramp. The flush type orifices were mounted along the center line of the ramp.

## TESTS

The pressure recoveries at the duct center line were measured for each of four outlet constrictions (various mass-flow ratios) at constant Mach numbers in the range 0.50 to 1.10. Typical curves of the measured ram-recovery ratios  $\frac{H_1 - p_0}{H_0 - p_0}$  across the inlet entrance are presented in figure 6.

The variation of mass-flow ratio with Mach number for two different outlet restrictions is presented in figure 7. Because of the variation in mass-flow ratio with Mach number, it was necessary to cross-plot the actual test data to obtain curves of ram-recovery ratio as a function of Mach number at constant values of mass-flow ratio.

## DISCUSSION

## Pressure-Recovery Characteristics

The variation of ram-recovery ratio with Mach number along the vertical center line of the inlet for constant mass-flow ratios from 0.3 to 0.6 is presented in figure 8.<sup>1</sup> Good recovery characteristics are indicated at the test mass-flow ratios up to test-station Mach numbers of 1.03 to 1.08. At some value of Mach number in this range, for mass-flow ratios below 0.5, the ram-recovery ratio<sup>2</sup> decreased abruptly.

The abrupt loss in ram-recovery ratio at the higher Mach numbers obtained in this investigation of an aspect ratio 5 inlet is believed to be due to separation along the ramp caused by shock-wave boundary-layer interaction. During a run with gradually increasing test-station Mach number the occurrence of a shock wave on the inlet ramp was indicated. Figure 9 shows the variation of local Mach number over the forward portion of the ramp for several values of test-station Mach number and for two mass-flow ratios taken during this run. At a test-station Mach number of approximately 1.05, a shock wave occurred on the inlet ramp as indicated by the abrupt change in local Mach number. This abrupt change occurred, with no change in inlet geometry, simultaneously with the loss in ram-recovery ratio and mass-flow ratio shown in figure 10. It will be seen from figure 10 that when the loss occurred it was distributed across the entire height of the inlet. This indicates considerable thickening of the boundary layer and separation due to the interaction of the ramp boundary layer and shock wave.

---

<sup>1</sup>These values are the average and are not weighted according to the local mass-flow ratio.

<sup>2</sup>It should be noted that the ram-pressure recoveries presented in this report do not represent the total inlet characteristics, but represent conditions only along the center line of the inlet.

---

A further indication of the effect of this ramp shock wave is evident in the variation of mass-flow ratio with Mach number. In figure 7, for one particular configuration, a decrease of 0.113 mass-flow ratio occurred at a Mach number of 1.08 when the shock wave appeared on the entrance ramp.

#### Application of Data to Fuselage Installations

The effect of the ramp boundary-layer and shock-wave interaction on the variation of pressure recovery with Mach number is a significant factor in evaluating the results of these tests of an isolated inlet. Quantitative comparisons with other tests or use of the data to estimate the characteristics of an installation on a fuselage not only must be made for the same aspect ratio but will accurately represent conditions only for locations having static-pressure gradients, superstream velocities, and boundary-layer characteristics similar to the wing-flow test station.

A comparison between the Mach number gradients over the wing-flow test station and those over a prolate spheroid of fineness ratio of 6 is presented in figure 11. The data for the prolate spheroid were obtained from reference 5. This comparison is made for a reference Mach number of 0.95. The variations at other Mach numbers were such that the relation shown in figure 11 is considered to be representative of the comparison between the wing-flow test station and a prolate spheroid of fineness ratio of 6. It can be concluded from figure 11 that the pressure gradient and superstream velocities existing at the ramp location on the wing-flow test station approximate those existing between the 16-percent to 36-percent stations on the prolate spheroid. Thus, except for differences in boundary-layer characteristics (due to differences between two- and three-dimensional effects as well as those arising from scale), the test data of this report can be considered to represent the characteristics of a flush inlet configuration such as pictured at the top of figure 11.

#### CONCLUDING REMARKS

Measurements conducted on a wing-flow-method test station have been used to study the effect of Mach number on the pressure-recovery characteristics of an NACA submerged inlet of aspect ratio 5. The favorable low-speed characteristics were maintained up to the Mach number range 1.03 to 1.08 where, for mass-flow ratios below 0.5, an abrupt loss in pressure recovery was measured. This abrupt loss in ram-recovery ratio is believed to be due to separation along the ramp caused by shock-wave boundary-layer interaction.

In any attempt to use these results it is important to take into consideration that they are subject to influence not only by the given inlet geometry (e.g., inlet aspect ratio, ramp divergence, etc.), but also by the pressure field existing on the basic body, which will influence boundary-layer growth, separation, and superstream velocities along the ramp.

Ames Aeronautical Laboratory,  
National Advisory Committee for Aeronautics,  
Moffett Field, Calif.

#### REFERENCES

1. Mossman, Emmet A., and Randall, Lauros M.: An Experimental Investigation of the Design Variables for NACA Submerged Duct Entrances. NACA RM A7I30, 1948.
2. Martin, Norman J., and Holzhauser, Curt A.: An Experimental Investigation at Large Scale of Several Configurations of an NACA Submerged Air Intake. NACA RM A8F21, 1948.
3. Hall, Charles F., and Frank, Joseph L.: Ram-Recovery Characteristics of NACA Submerged Inlets at High Subsonic Speeds. NACA RM A8I29, 1948.
4. Mossman, Emmet A.: A Comparison of Two Subsonic Inlets at Subsonic and Transonic Speeds. NACA RM A9F16, 1949.
5. Matthews, Clarence W.: Pressure Distributions over a Wing-Fuselage Model at Mach Numbers of 0.4 to 0.99 and at 1.2. NACA RM L8H06, 1948.

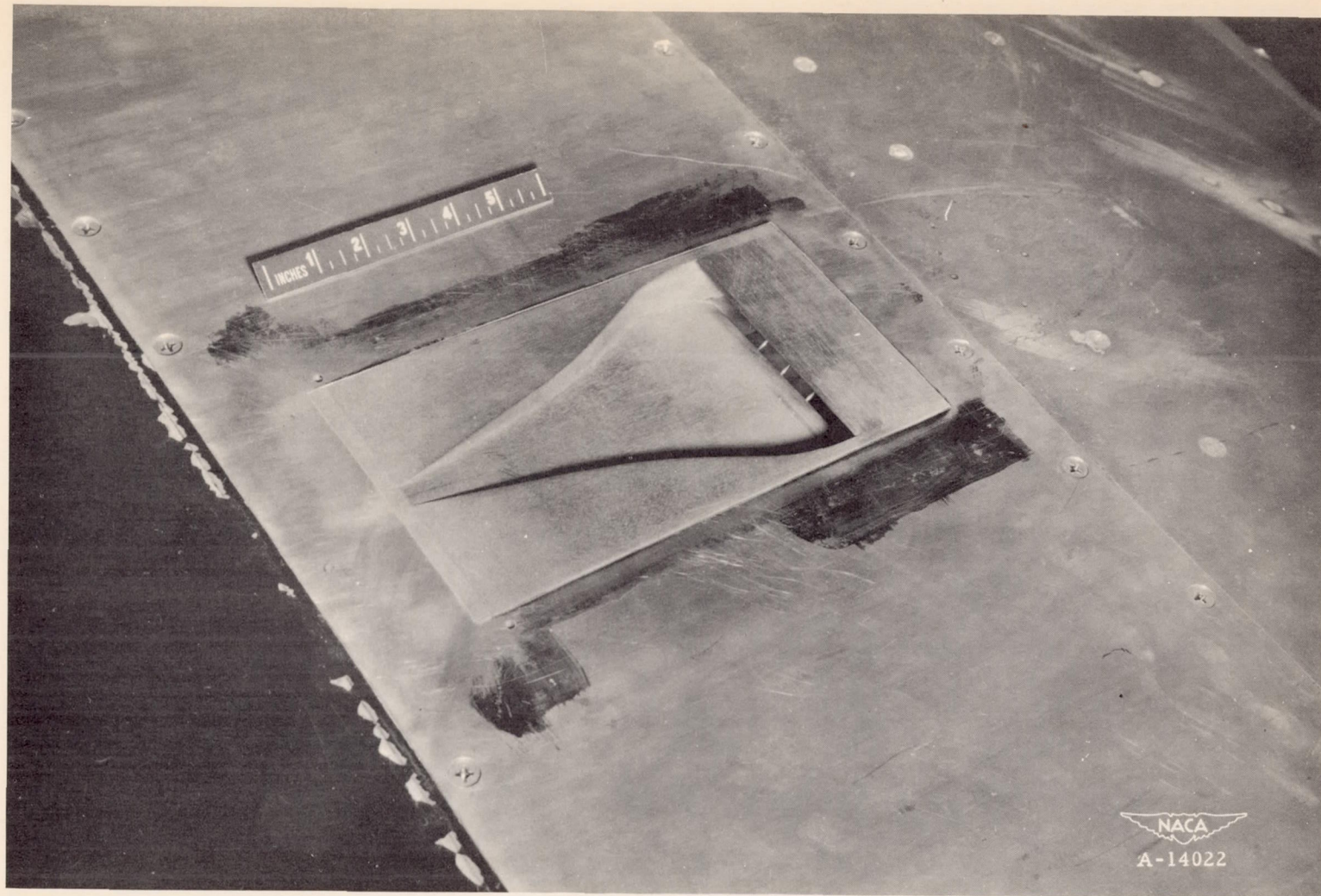
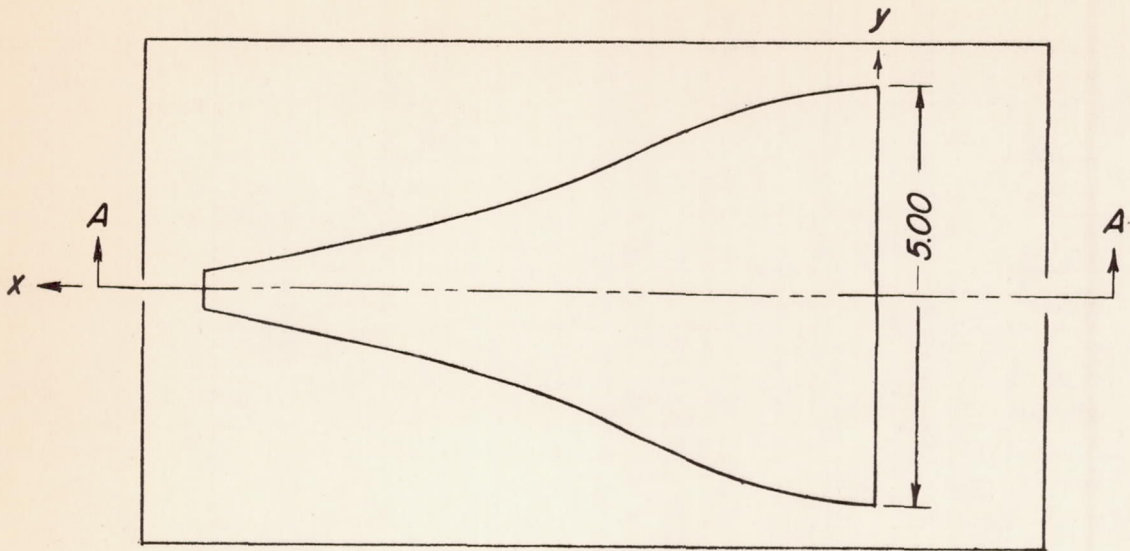


Figure 1.- General view of wing-flow test station with submerged inlet installed.





*Divergent wall ordinates*

<i>x</i>	<i>y</i>	<i>x</i>	<i>y</i>
0	2.500	4.840	0.980
0.805	2.470	5.640	0.780
1.610	2.290	6.440	0.590
2.420	1.910	7.240	0.400
3.220	1.540	8.050	0.210
4.030	1.210		

*All dimensions given are in inches*

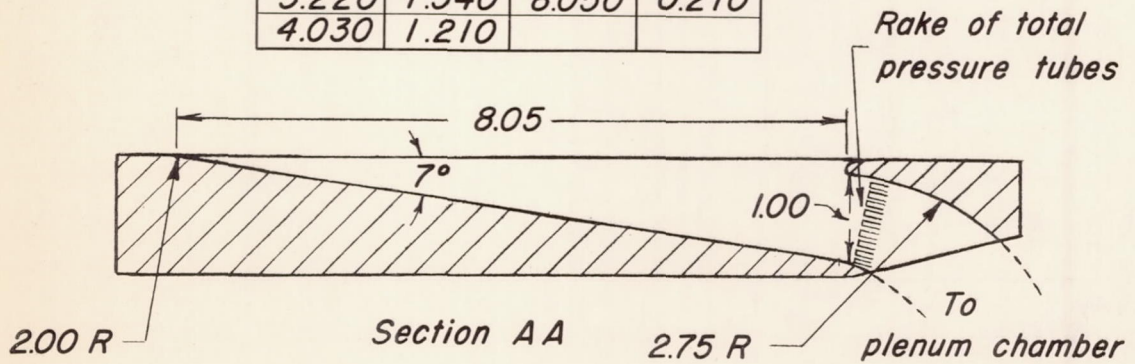


*Figure 2.- Drawing of submerged inlet.*

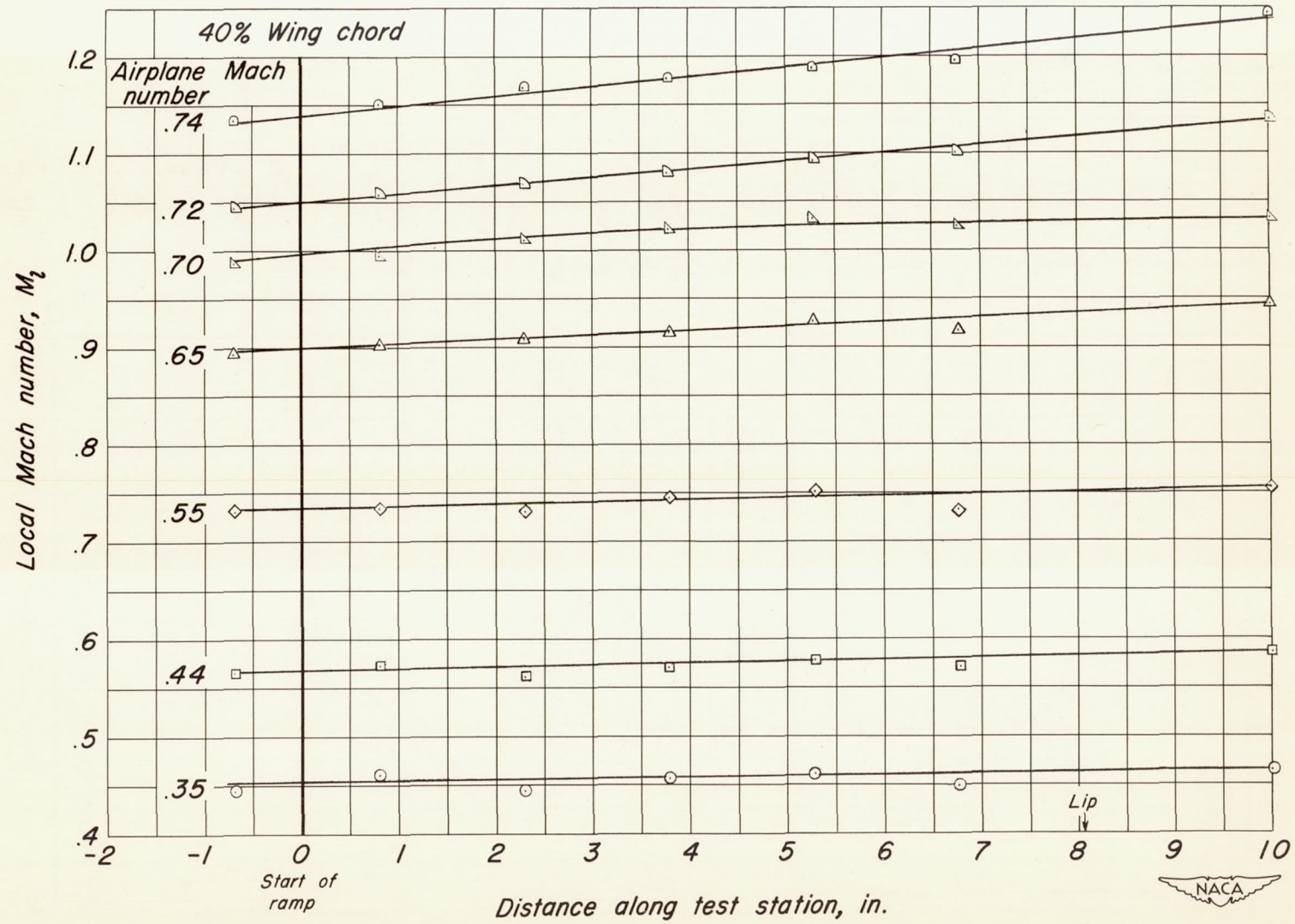


Figure 3.- Variation of Mach number along the wing-flow test station.

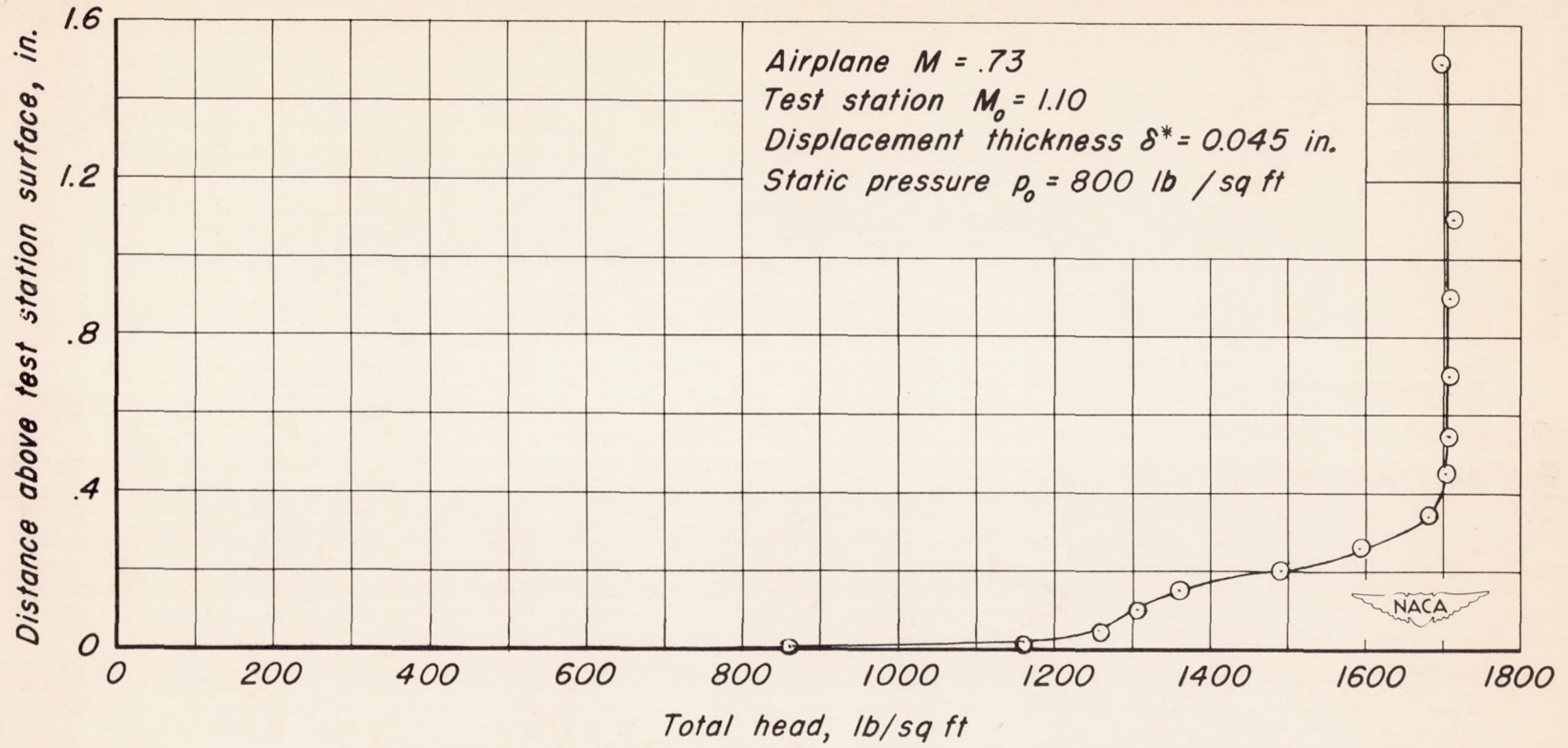


Figure 4.- Typical variation of total head through the boundary layer on the surface of the wing-flow test station.

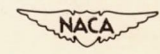
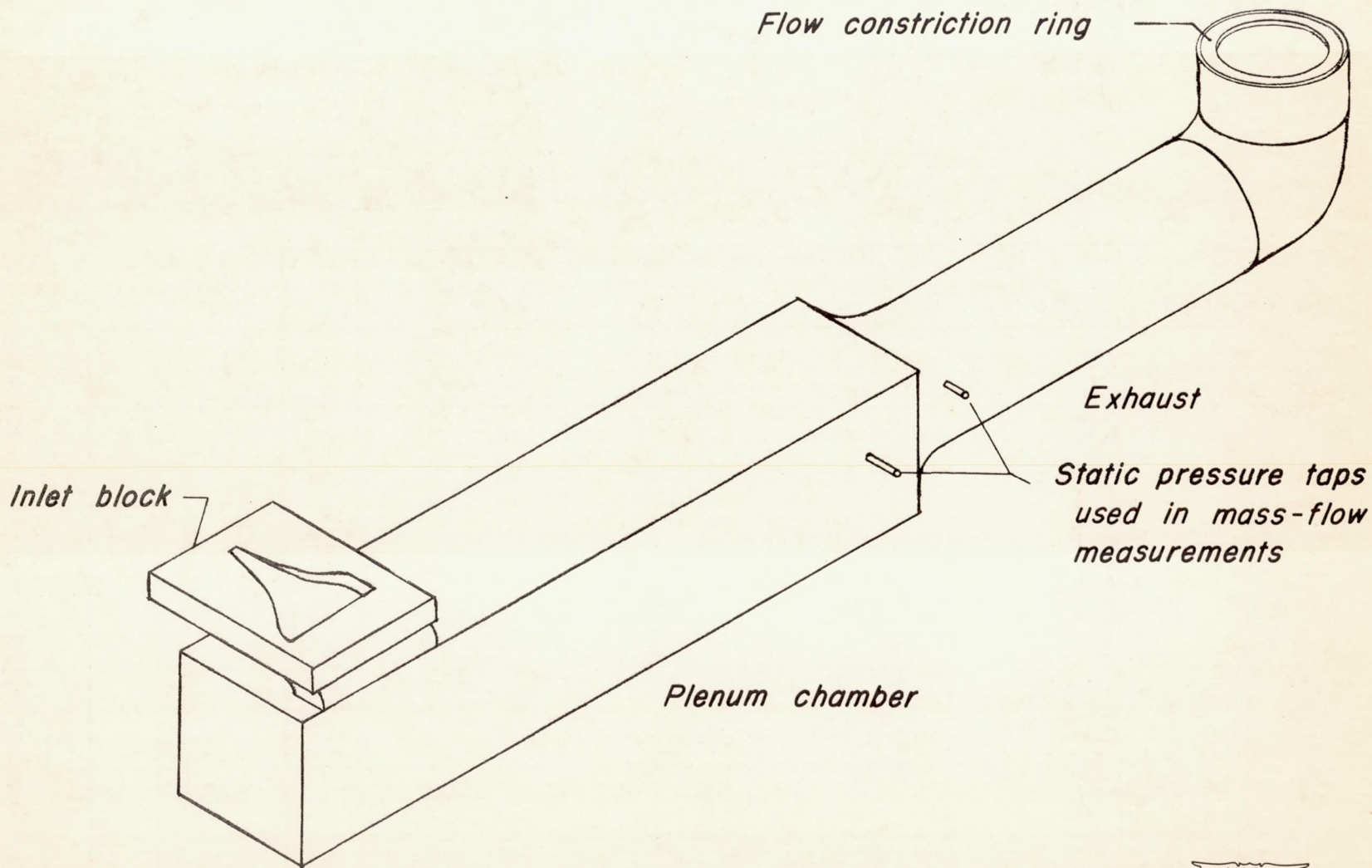


Figure 5.- Schematic drawing of inlet test assembly.

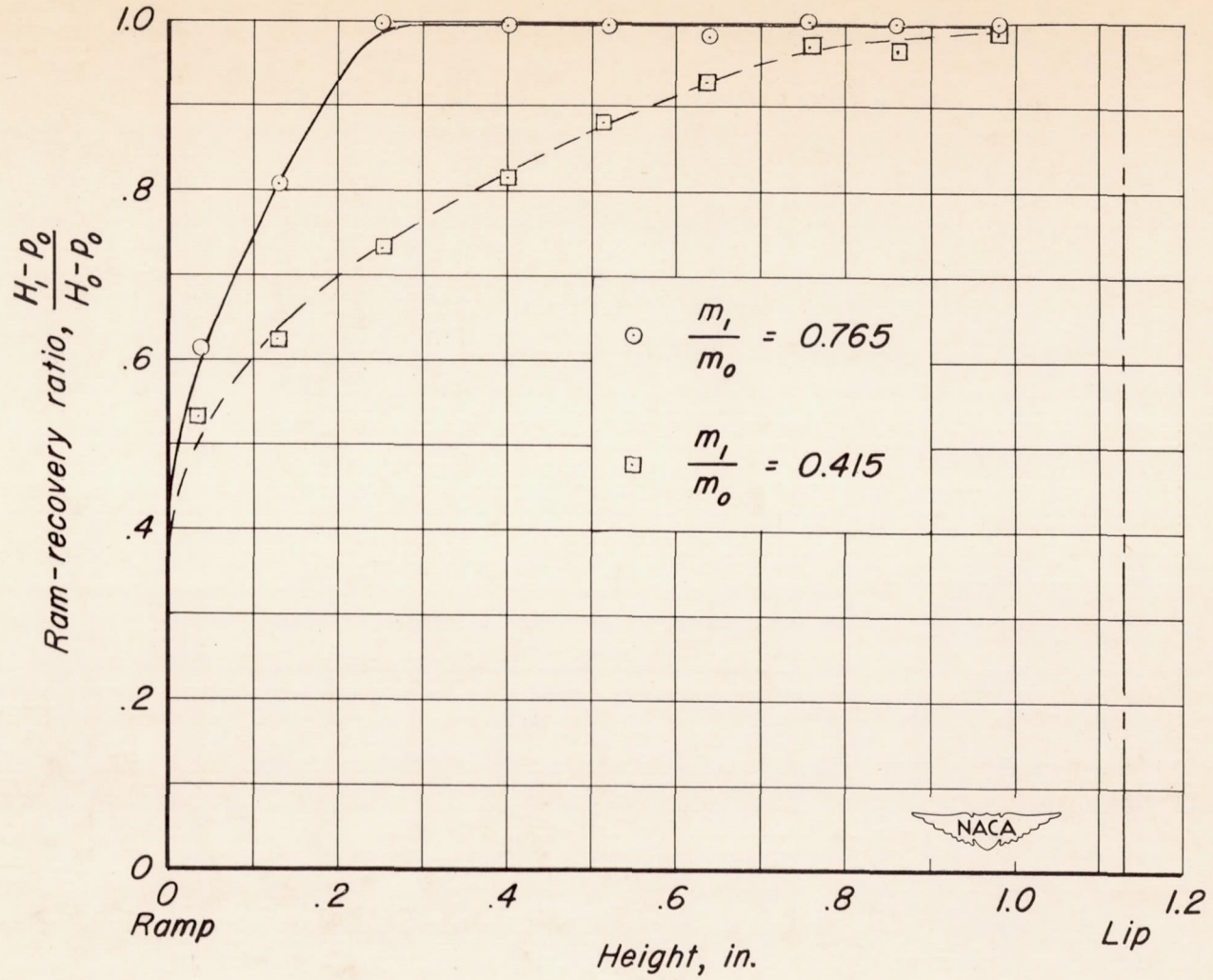


Figure 6.- Typical variations of ram-recovery ratio across the inlet measured at the center line.  $M_0 = 0.60$ .

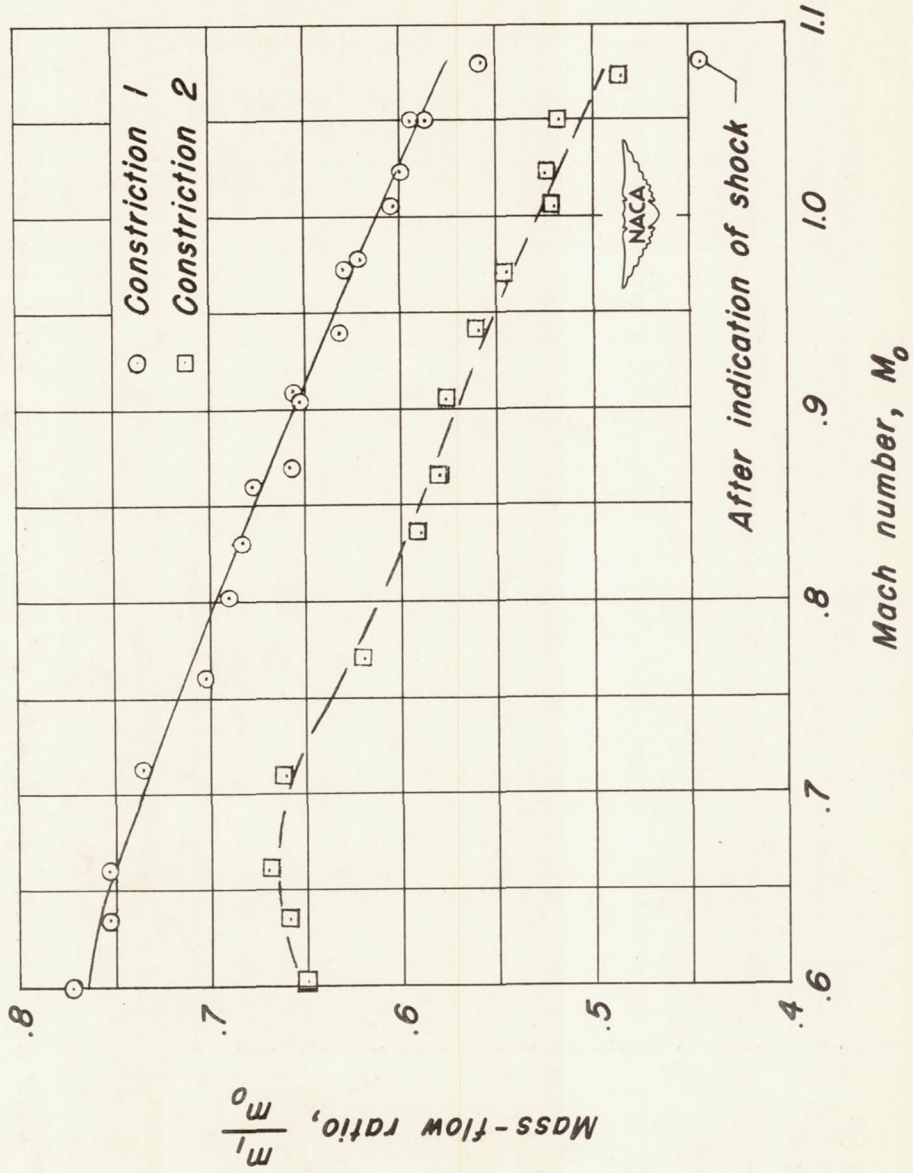


Figure 7. - Typical variations of mass-flow ratio with test station Mach number.

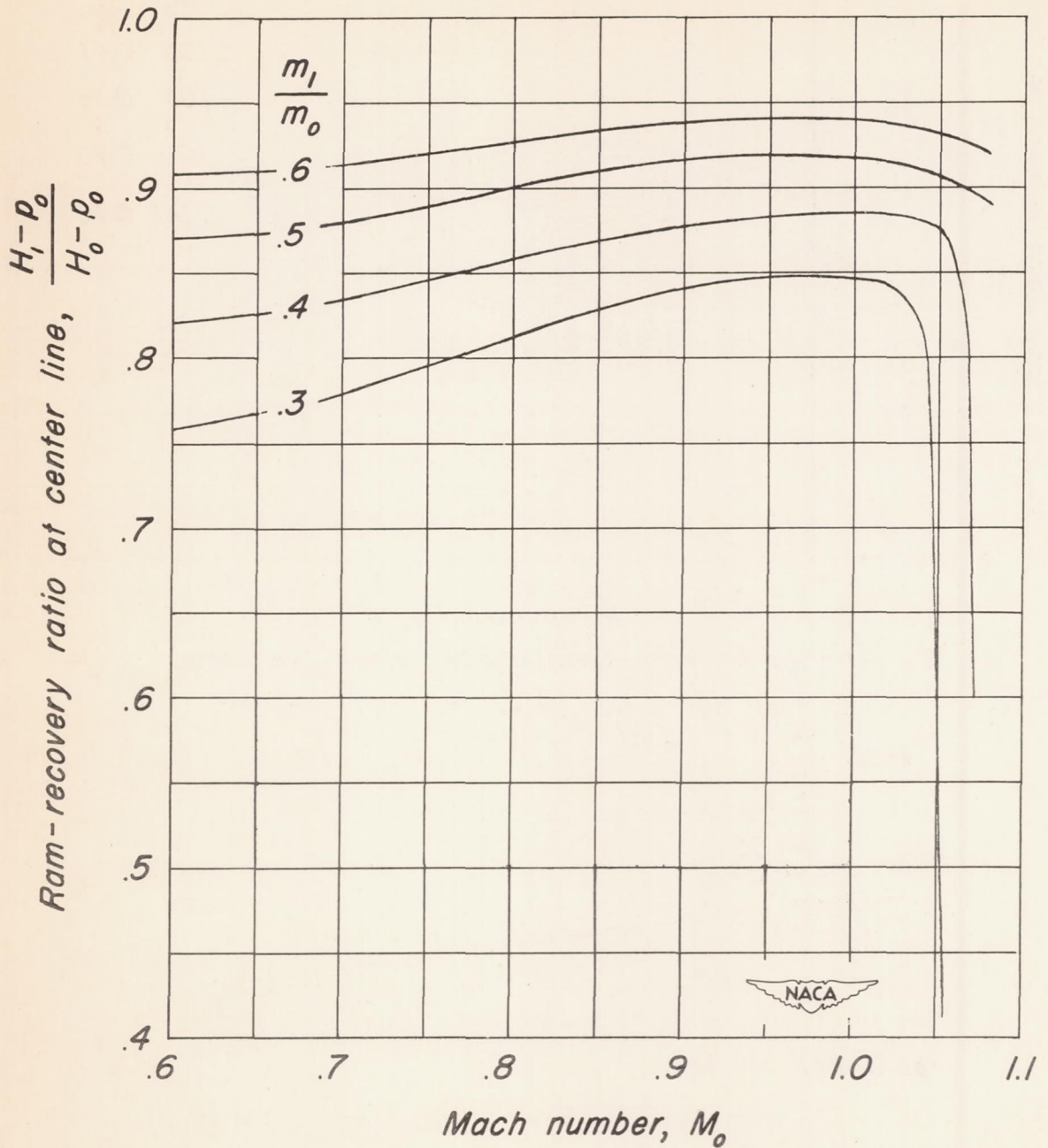
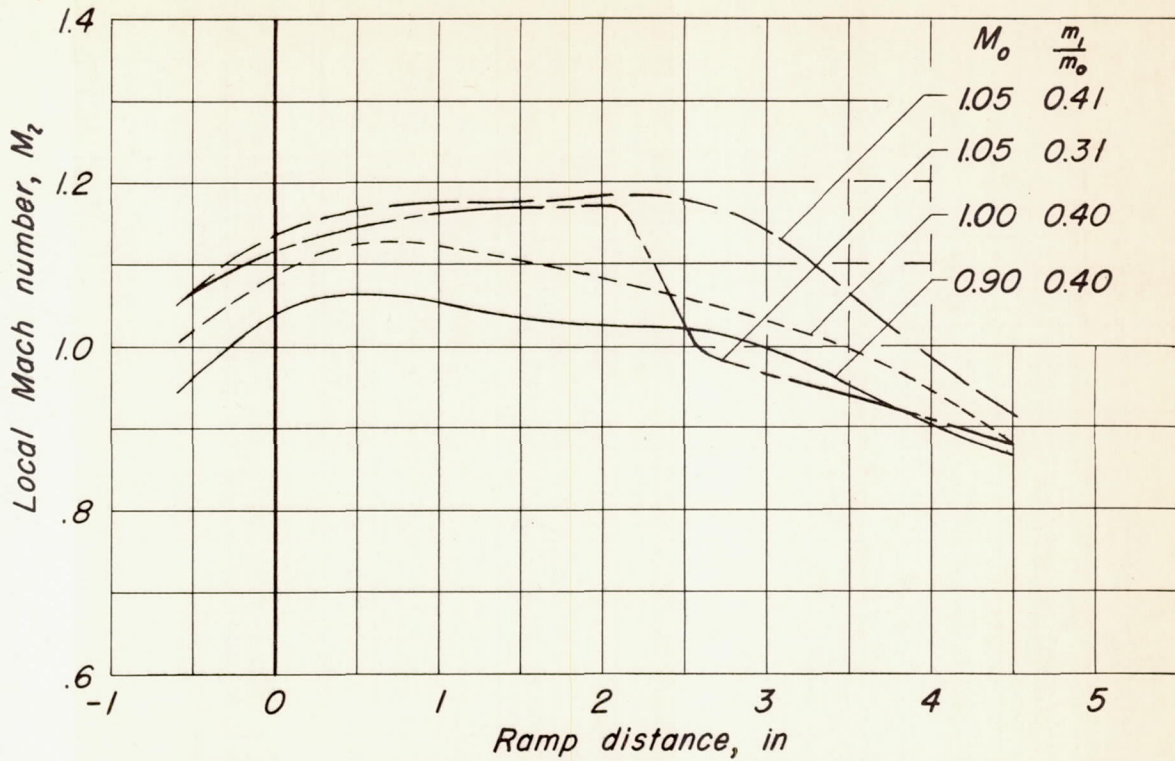
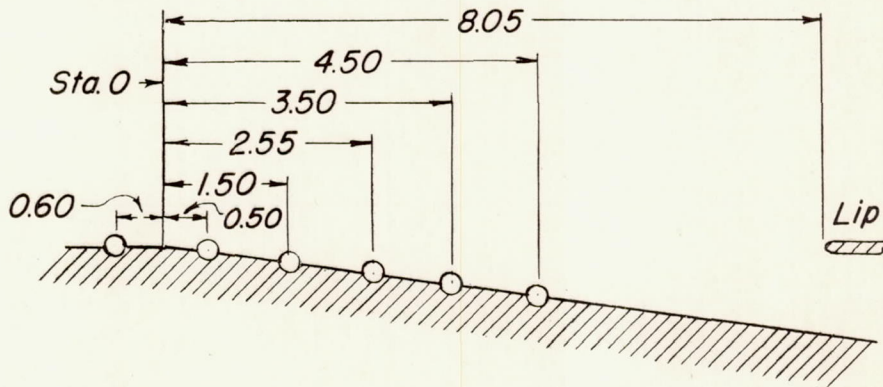


Figure 8.- Variation of ram-recovery ratio with Mach number for several values of mass-flow ratio.



(a) Variation of local Mach number along the ramp.



(b) Orifice locations.



Figure 9.- Mach number distribution along the inlet ramp as determined from static pressure orificies.

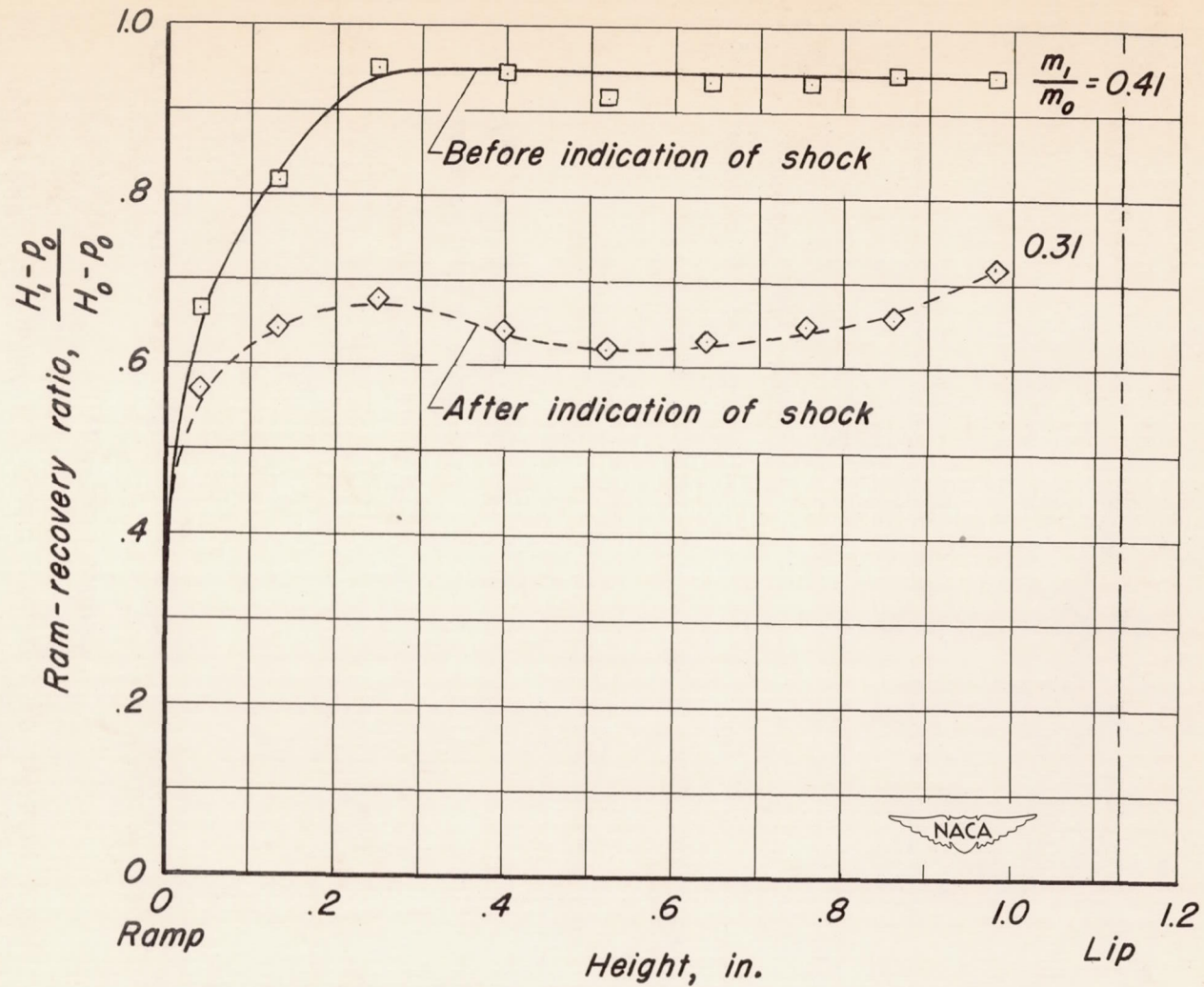


Figure 10.- Variation of ram-recovery ratio across the inlet before and after flow breakdown.  $M_0 = 1.05$ .

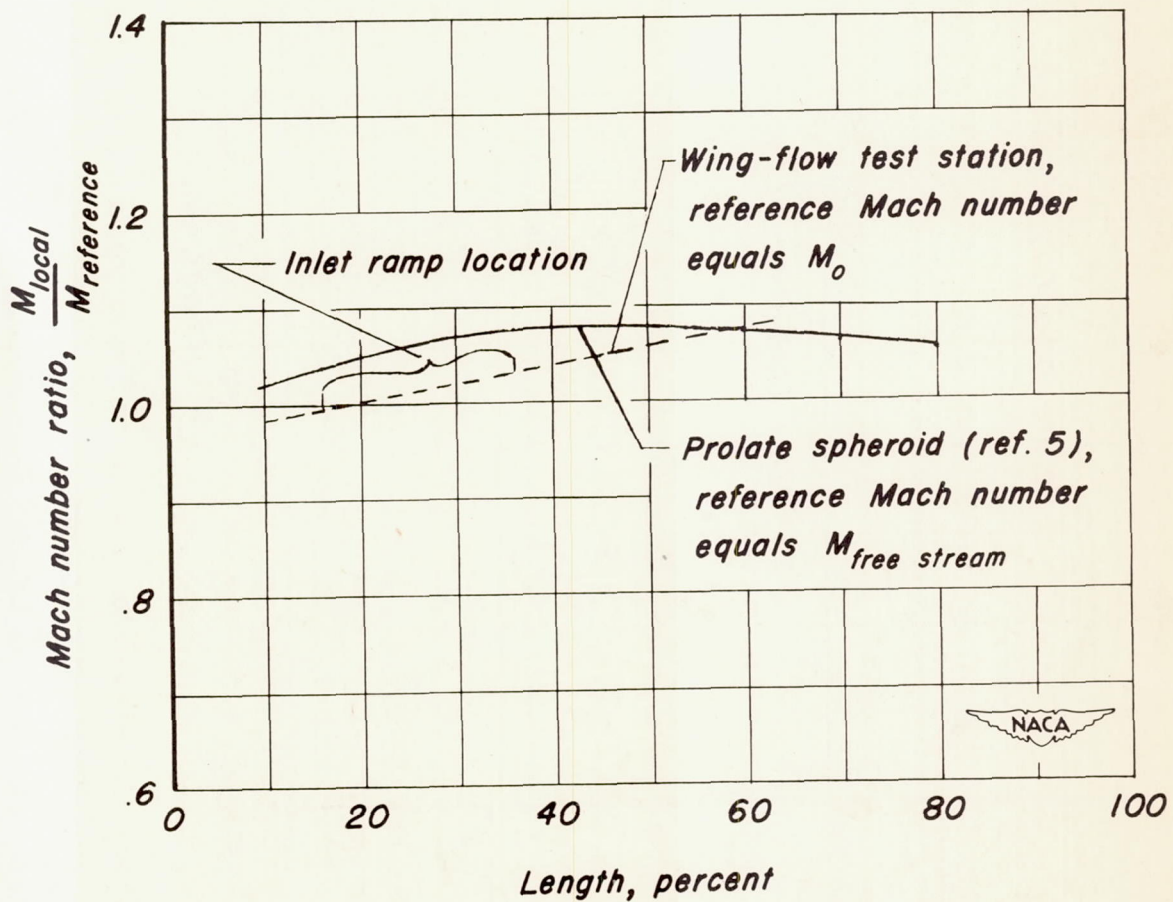
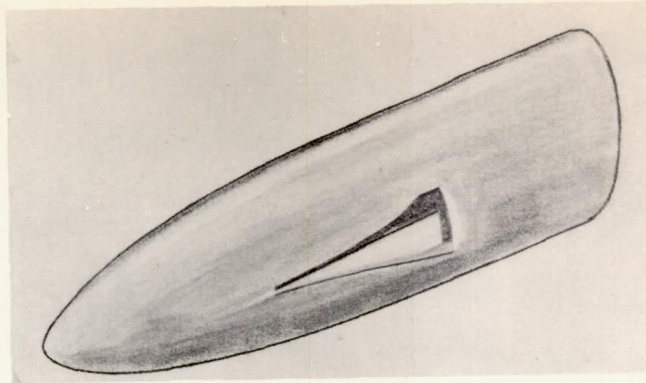


Figure 11.- The Mach number gradient along the body length for a body of revolution and the wing-flow test station. For a reference Mach number of 0.95.